

O-H wag vibrations in hydrated $\text{BaIn}_x\text{Zr}_{1-x}\text{O}_{3-x/2}$ investigated with inelastic neutron scatteringMaths Karlsson,^{1,*} Aleksandar Matic,¹ Stewart F. Parker,² Istaq Ahmed,³ Lars Börjesson,¹ and Sten Eriksson³¹*Department of Applied Physics, Chalmers University of Technology, SE-412 96 Göteborg, Sweden*²*ISIS Facility, STFC Rutherford-Appleton Laboratory, Chilton, Didcot OX11 0QX, United Kingdom*³*Department of Chemical and Biological Engineering, Chalmers University of Technology, SE-412 96 Göteborg, Sweden*

(Received 21 September 2007; revised manuscript received 7 February 2008; published 11 March 2008)

The nature of O-H wag vibrations in the cubic proton conducting perovskite-type oxides, $\text{BaIn}_x\text{Zr}_{1-x}\text{O}_{3-x/2}$ ($x=0.20-0.75$) have been investigated by means of inelastic neutron scattering. Our spectroscopic results show that the O-H wag vibrations are manifested as a broad band between 600 and 1300 cm^{-1} . With increasing In concentration, the O-H wag band increases in intensity and broadens with an increased weight of the high frequency part. The intensity increase of the O-H wag band is a result of the increasing concentration of protons in the perovskite structure while the increased weight of the high frequency part results from an increased fraction of protons in strongly hydrogen bonding configurations. Such strongly hydrogen bonding configurations of the proton is primarily a result of the presence of oxygen vacancies and dopant atoms, which act as charged defects, but also of local structural distortions caused by the introduction of dopant atoms. From the temperature dependence of the O-H wag band we find that the mean square displacement of the protons increases only slightly as the temperature is raised from 30 to 300 K, which implies that it is unlikely that the protons undergo long-range diffusion for temperatures below 300 K. Comparing the In concentration dependence of different components of the O-H wag band with the proton conductivity of the reported compositions indicates that protons in weak or intermediate hydrogen bonding configurations are likely the main charge carriers.

DOI: [10.1103/PhysRevB.77.104302](https://doi.org/10.1103/PhysRevB.77.104302)

PACS number(s): 78.70.Nx, 34.50.Ez, 82.47.Gh

I. INTRODUCTION

Ever since Takahashi and Iwahara^{1,2} showed that perovskite-type oxides can become proton conductors at elevated temperatures these materials have been intensively studied because of their potential to be used in various electrochemical applications.³ Most attention has been focused on simple perovskites, ABO_3 , although more complex perovskites, of e.g., the form $\text{A}_3(\text{B}'\text{B}'')\text{O}_9$, have also been investigated (here the A ion is divalent, the B ion is tetravalent, the B' ion is trivalent, and the B'' ion is pentavalent). Loading protons into these materials requires the formation of oxygen vacancies and subsequent hydration. For ABO_3 perovskites, the oxygen vacancies can be formed as a charge compensating effect by doping with lower-valent ions M^{3+} to the B^{4+} site, while for the complex perovskites of type $\text{A}_3(\text{B}'\text{B}'')\text{O}_9$, the oxygen vacancies can be formed by changing the stoichiometric ratio of the divalent B' ion and the pentavalent B'' ion. The general formulas for these two types of oxygen deficient perovskites can be written as $\text{AB}_{1-x}\text{M}_x\text{O}_{3-x/2}$ and $\text{A}_3(\text{B}'_{1+x}\text{B}''_{2-x})\text{O}_{9-3x/2}$, respectively. Hydration of these materials is generally performed by annealing in a humid atmosphere at elevated temperatures. During this procedure, water molecules dissociate into hydroxide ions which fill the oxygen vacancies while each of the remaining protons forms a covalent bond with one individual lattice oxygen.³

Supported by several independent neutron scattering experiments⁴⁻⁶ and simulations⁷⁻¹⁰ it is suggested that the proton transport in these materials occurs through two elementary steps: (i) proton transfer between neighboring oxygens via hydrogen bonds, and (ii) rotational motion of the hydroxyl group in-between such transfers.³ Precursors to the elementary processes are the vibrational motions of the pro-

tons in these systems, namely, O-H stretches and O-H wags. The frequencies of these modes are commonly used as pre-factors in transition state models to estimate the rates of the proton transfer and reorientational steps, respectively.¹¹ The O-H stretch vibrations are clearly observable with infrared (IR) spectroscopy, where they are manifested as a strong band between 2500 and 3500 cm^{-1} .^{12,13} The broad nature of this band results from a distribution of hydrogen bond strengths between the proton and a neighboring oxygen (O-H \cdots O). The presence of a hydrogen bond increases the O-H bond distance, which lowers the O-H stretch frequency. We have previously shown that nonsymmetrical configurations of the protons, such as sites close to dopant atoms and/or oxygen vacancies, result in an enhanced tendency for hydrogen bond formation.¹³ Therefore, the low and high frequency parts of the broad O-H stretch band have been suggested to be related to protons in relatively nonsymmetrical and symmetrical configurations, respectively.¹³

In contrast to the O-H stretch mode, the O-H wag mode is not at all well investigated. The reason for this is the very weak IR and Raman activity of the O-H wag vibration, which makes it difficult to study with conventional light spectroscopy. In inelastic neutron spectroscopy (INS), however, the O-H wag vibrations give rise to a strong band due to the large scattering cross section of hydrogen. Therefore, it is surprising that, at least to our knowledge, there is only one report on the INS spectra of hydrated perovskites.¹⁴ This experiment was performed on the orthorhombic perovskite system $\text{SrCe}_{0.95}\text{M}_{0.05}\text{O}_{3-\delta}$ ($M=\text{Sc}, \text{Ho}, \text{Nd}$), and revealed two O-H wag bands, at ~ 600 and ~ 900 cm^{-1} , of which the high frequency band was associated with protons close to dopant atoms.¹⁴ Moreover, in a temperature study of the Sc-doped material, it was shown that the dopant-related band disap-

peared into the background for temperatures above 200 K, which was interpreted as a delocalization of dopant-related protons.¹⁴ However, neither an investigation of the dopant level dependence nor any relation to the corresponding O-H stretch vibrations was made. This information is important in order to understand the details of the proton conduction mechanism in hydrated perovskites and ultimately be able to systematically guide the synthesis of materials with higher proton conductivity.

In this work we investigate the O-H wag vibrations in hydrated $\text{BaIn}_x\text{Zr}_{1-x}\text{O}_{3-x/2}$ ($x=0.20-0.75$), using INS. As determined from x-ray and neutron diffraction experiments, $\text{BaIn}_x\text{Zr}_{1-x}\text{O}_{3-x/2}$ ($x=0.20-0.75$) has an average cubic structure (space group $Pm\bar{3}m$) with lattice parameter $a_{\text{perov}}=4.19-4.25$ Å, and with the dopant atoms randomly distributed over the B site.¹⁵⁻¹⁹ The fact that the average cubic symmetry remains over the large dopant range allows us to systematically investigate the effect of the dopant level on the O-H wag mode without any influence of large structural changes. We also investigate the effect of temperature within the range 30–300 K, and the difference between hydrated and dry materials. The results are compared to the development of the corresponding O-H stretch band,¹³ to the previously reported INS study of hydrated perovskites,¹⁴ and to the proton conductivities as reported elsewhere.^{17,18}

II. INELASTIC NEUTRON SCATTERING

In an INS experiment, the measured intensity of a vibrational band, S_i , is a function of both the energy transfer $\hbar\omega$, and the momentum transfer Q , exchanged during the scattering process, and is proportional to²⁰

$$S_i(Q, \omega) \propto \frac{(QU_i)^{2n}}{n!} \sigma e^{-Q^2 U_T^2}. \quad (1)$$

Here, $n=1$ for a fundamental mode, $n=2$ for the first overtone, $n=3$ for the second overtone, etc. U_i is the vibrational amplitude of the normal mode i , σ is the neutron scattering cross sections of all atoms involved in the mode, and U_T is the total root mean square displacement of these atoms summed over all modes.²⁰ The exponential factor in Eq. (1) is known as the Debye-Waller factor, which at high Q values always suppresses the intensity more than the preexponential factor increases. Furthermore, as U_T usually increases significantly with temperature, the measurements are generally performed at low temperature (≤ 50 K) in order to minimize damping of the vibrational bands.

One should note that the neutron cross section for hydrogen is ~ 80 b, which is by far larger than for any other element of typical perovskites which have cross sections smaller than 7 b.²¹ Provided that the hydrogen concentration is not very low, this implies that the vibrations involving hydrogen will dominate the spectrum. The cross section dependence in INS is the reason why this technique is so different from optical vibrational spectroscopy, Raman and infrared, which rely on certain selection rules (change in electronic polarizability and dipole moment, respectively).²² In INS all vibrational modes are active and, in principle, measurable.

III. EXPERIMENT

A. Sample preparation

The samples were prepared through traditional solid state sintering. Since as-prepared samples are known to contain some protons the dehydrated (dry) sample was prepared by annealing the as-prepared samples under vacuum ($\sim 2 \times 10^{-6}$ mbar) at 950 °C overnight to remove as many protons as possible. The loading with protons was performed by annealing the as-prepared samples at 275–300 °C under a flow (12 ml/min) of Ar saturated with water vapor at 76 °C for ten days. X-ray diffraction of the dry and hydrated samples revealed the cubic symmetry for all materials with lattice parameters $a=4.1996(1)$ Å for $\text{BaIn}_{0.20}\text{Zr}_{0.80}\text{O}_{2.90}$, $a=4.2018(3)$ Å for $\text{BaIn}_{0.50}\text{Zr}_{0.50}\text{O}_{2.75}$, and $a=4.2125$ Å for $\text{BaIn}_{0.75}\text{Zr}_{0.25}\text{O}_{2.625}$ in agreement with our previous structural investigations.¹⁷ Further details of the sample preparation procedure can be found elsewhere.¹⁷

B. Inelastic neutron scattering

The INS experiments were performed at the inverse geometry time-of-flight spectrometer TOSCA at the ISIS pulsed spallation neutron source at the Rutherford Appleton Laboratory, Chilton, Didcot, Oxfordshire, UK. The TOSCA spectrometer, described in detail in Refs. 23 and 24, makes use of ten detector banks, five viewing the forward scattering ($\sim 47.50^\circ$) and five viewing the backward scattering ($\sim 132.30^\circ$).²³ At TOSCA it is, in principle, possible to measure vibrational modes over a range of approximately $\omega = 16-4000$ cm^{-1} , with an energy resolution of about 1.25% of the energy transfer. However, the design of the spectrometer is such that Q increases with ω , implying that the high frequency part of the INS spectra are strongly damped by the Debye-Waller factor [see Eq. (1)].

The samples were ground to fine powders and loaded in vacuum tight containers of Al with a sample thickness of 3–5 mm, corresponding to a total scattering of neutrons of about 10%. The beam size at the sample was 40 mm high by 40 mm wide. INS spectra were measured at 30 K for all compositions, and at 100, 200, and 300 K for $x=0.20$. The sample temperature was controlled using a closed cycle refrigerator (CCR), and for the heating experiment heating blocks were mounted on the sample container. For each sample the measurement time was approximately 6 h. The INS spectra are presented as the scattering function $S(Q, \omega)$ versus energy transfer in units of wave numbers (cm^{-1}), and are the sum of the forward and the backward scattering. The spectra are normalized by $n(\omega)+1$, where $n(\omega)$ is the Bose-Einstein statistical occupation factor given by

$$n(\omega) = \frac{1}{\exp\left(\frac{\hbar\omega}{k_B T}\right) - 1}. \quad (2)$$

IV. RESULTS

Figure 1 shows the INS spectra, 50–2000 cm^{-1} , of hydrated $\text{BaIn}_x\text{Zr}_{1-x}\text{O}_{3-x/2}$ with $x=0.20, 0.50$, and 0.75, and dry

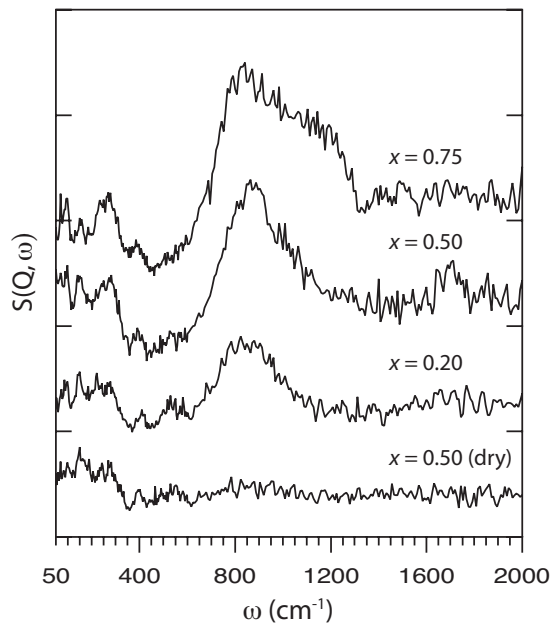


FIG. 1. INS spectra of hydrated $\text{BaIn}_x\text{Zr}_{1-x}\text{O}_{3-x/2}$ ($x=0.20, 0.50$, and 0.75) and dry $\text{BaIn}_x\text{Zr}_{1-x}\text{O}_{3-x/2}$ ($x=0.50$) at 30 K. The spectra have been vertically offset for clarity.

$\text{BaIn}_x\text{Zr}_{1-x}\text{O}_{3-x/2}$ with $x=0.50$, measured at 30 K. The spectra of the hydrated materials are dominated by a strong and broad band between 600 and 1300 cm^{-1} , which gradually grows in intensity and gets broader with increasing In concentration. The fact that this band is absent in the spectra of the dry material but very strong in the spectra of the hydrated materials shows that it is related to vibrational motions of the protons in the structure. Based on the fact that the band is located at considerably lower frequencies than the O-H stretch band ($2500\text{--}3500\text{ cm}^{-1}$),¹³ and at higher frequencies than the host-lattice vibrations of the perovskite, found below 800 cm^{-1} (see below), we assign this band to the O-H wag vibrations. This assignment also agrees well with first-principles calculations, which suggest contributions from O-H wag vibrations in the range of $500\text{--}1100\text{ cm}^{-1}$ for this perovskite system.¹³

In the spectra of the hydrated materials a broad feature, centered at around 1700 cm^{-1} , is also observed. This band is, most likely, related to the first overtone of the fundamental O-H wag band, located at approximately half this vibrational frequency. Apart from the frequencies of these two bands, this assignment is further supported by the fact that their shapes are similar. For instance, for $x=0.50$, both the fundamental band and its overtone are relatively sharp and intense, while, for $x=0.75$, the overtone band is more smeared out due to the broad nature of the corresponding fundamental band.

At lower frequencies, $50\text{--}600\text{ cm}^{-1}$, the spectra of the hydrated materials and the dry material are very similar to each other and exhibit a series of sharper bands. Specifically, we observe bands at around $70, 90, 150, 190, 240, 270, 400$, and 530 cm^{-1} . A comparison with our Raman and IR data on the same materials suggests that these bands are related to various vibrational modes of the host lattice of the perovskite.²⁵ The Raman and IR bands are found at 70 (Ra-

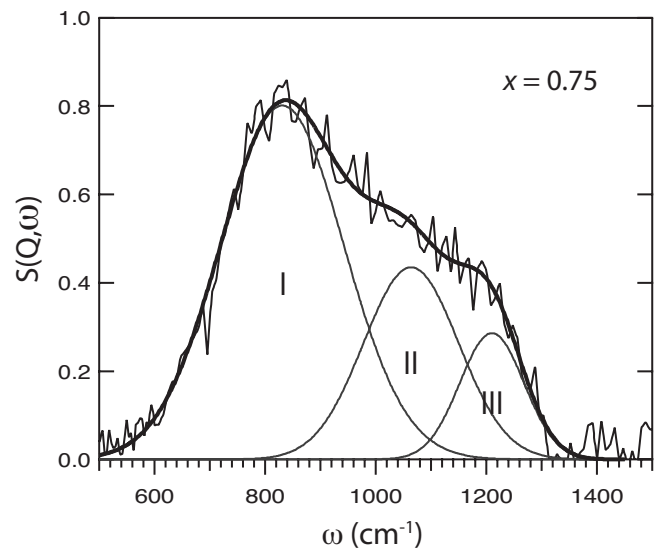


FIG. 2. Gaussian fit of the baseline corrected O-H wag band for hydrated $\text{BaIn}_x\text{Zr}_{1-x}\text{O}_{3-x/2}$ ($x=0.75$).

man), 90 (Raman), 130 (Raman/IR), 200 (IR), 250 (Raman), $250\text{--}350$ (IR), 400 (Raman/IR), $500\text{--}700$ (IR), 550 (Raman), and 680 cm^{-1} (Raman), which agree well with the low frequency INS bands in Fig. 1.

In order to quantitatively assess the changes of the O-H wag band with In concentration in Fig. 1, we have fitted the spectra using a minimum number of Gaussian bands in the range $500\text{--}1400\text{ cm}^{-1}$ after subtracting a linear baseline. In this way, the $x=0.20$ spectrum could be well reproduced by two Gaussians at ~ 850 and $\sim 1070\text{ cm}^{-1}$, while the spectra for $x=0.50$ and $x=0.75$ required one additional component, at $\sim 1250\text{ cm}^{-1}$, to reproduce the profile of the O-H wag band. Figure 2 shows the fit for $\text{BaIn}_x\text{Zr}_{1-x}\text{O}_{3-x/2}$ with $x=0.75$ as an example and in Fig. 3 the peak frequency and relative intensity of the three Gaussian bands (marked with Roman numerals), and the total intensity of the O-H wag band as obtained from the sum of the three Gaussians, are shown as a function of composition. The widths of the Gaussians do not change with composition within the statistical uncertainty and are therefore not shown. As seen in Fig. 3(a), band III shifts toward lower wave numbers with In concentration while the position of band I and band II basically does not change. Furthermore, from Fig. 3(b) we see that the relative intensity of band I decreases linearly and the relative intensities of bands II and III increase gradually with the In concentration. Finally, as shown in Fig. 3(c), the total intensity of the O-H wag band increases linearly with In concentration and extrapolates perfectly to zero for the undoped material.

Regarding the effect of temperature increase on the O-H wag band, Fig. 4 shows the INS spectra of hydrated $\text{BaIn}_x\text{Zr}_{1-x}\text{O}_{3-x/2}$ ($x=0.20$) measured at $T=30, 100, 200$, and 300 K . The spectra have been corrected by the temperature dependent multiphonon contributions, as were calculated using the same method as Li *et al.*²⁶ As seen in Fig. 4, the only effect on the one-phonon spectra up to 200 K is a slight symmetric broadening of the O-H wag band with increasing temperature, while for the 300 K spectrum the broadening is more pronounced.

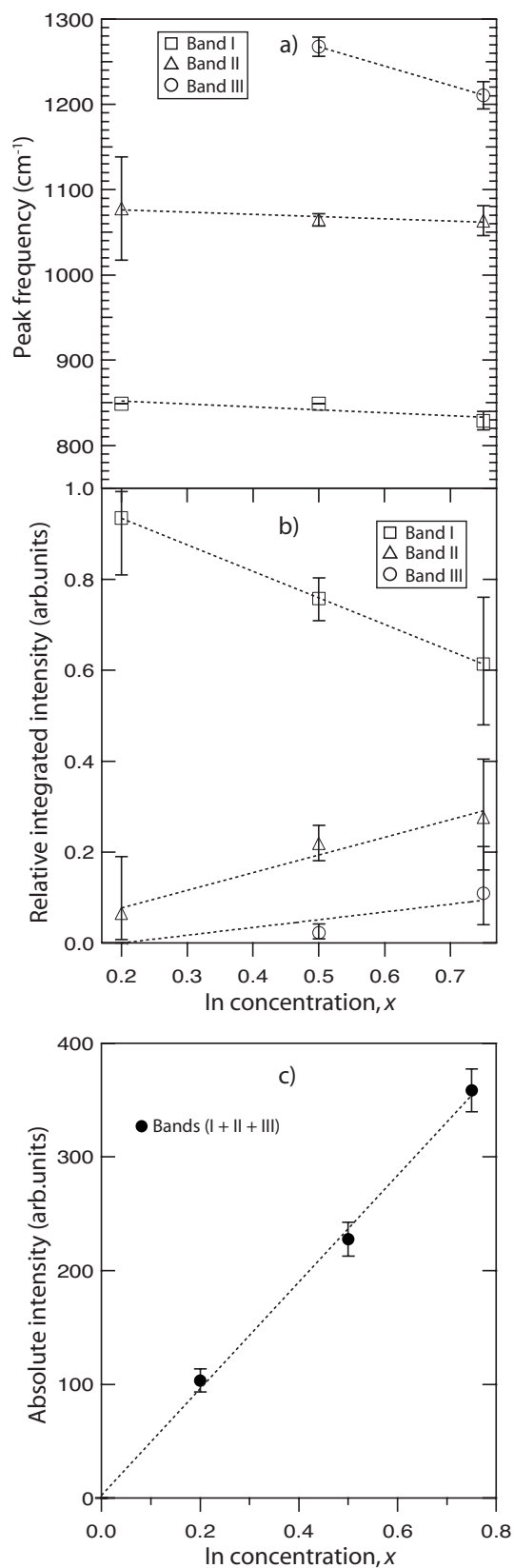


FIG. 3. Fit parameters: (a) and (b) show the peak positions and relative integrated intensities of the three Gaussian bands. (c) shows the sum of the integrated intensities of the three Gaussians, i.e., the total intensity of the O-H wag band. Linear fits serve as guides for the eye. In (c), the fit has been extrapolated to $x=0$.

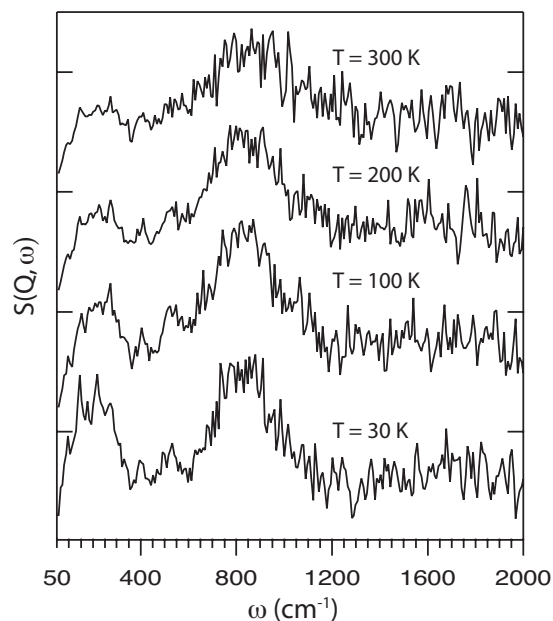


FIG. 4. Temperature dependence of the INS spectra of hydrated $\text{BaIn}_x\text{Zr}_{1-x}\text{O}_{3-x/2}$ ($x=0.20$). The spectra have been vertically offset for clarity.

V. DISCUSSION

Our INS results clearly show that the O-H wag vibrations in the hydrated perovskite system $\text{BaIn}_x\text{Zr}_{1-x}\text{O}_{3-x/2}$ ($x=0.20-0.75$) are manifested as a broad band between 600 and 1300 cm⁻¹ in the spectra. The total intensity of the O-H wag band is directly related to the number of protons in the material. Thus, the fact that the intensity of the O-H wag band increases linearly with increasing In concentration [see Fig. 3(c)] shows that the degree of hydration is the same for the investigated compositions. This result agrees well with the report by Kreuer *et al.*, where it was found from thermal gravimetric analysis (TGA) that the hydration degree of a similar perovskite system, $\text{BaY}_x\text{Zr}_{1-x}\text{O}_{3-x/2}$ ($x=0.02-0.25$), differed only slightly amongst the different dopant concentrations.²⁷ Those researchers also measured the hydration degree in $\text{BaIn}_x\text{Zr}_{1-x}\text{O}_{3-x/2}$ ($x=0.10$), which was determined to be approximately 60%.²⁷ Based on these results, it is reasonable to assume that hydrated $\text{BaIn}_x\text{Zr}_{1-x}\text{O}_{3-x/2}$ ($x=0.20-0.75$) is not fully hydrated but contains a significant amount of oxygen vacancies, and that the number of oxygen vacancies increases linearly with dopant concentration.

For $x=0.20$, the O-H wag band can be reproduced by two Gaussian bands at approximately 850 and 1070 cm⁻¹, respectively, while the fits for the higher In concentrations require one additional component located at a higher frequency, ~ 1250 cm⁻¹. It is seen from the relative intensities of these bands (Fig. 3) that the change in shape of the O-H wag band with increasing In concentration results from an increased weight of the two high frequency components. Interestingly, this corresponds well to a simultaneous broadening and increased weight of the low frequency part of the corresponding O-H stretch band between 2500 and 3500 cm⁻¹ for the same perovskite system.¹³ The shapes of

the O-H stretch and O-H wag bands for the different In concentrations are, in fact, well mirrored by each other. This shows that the frequency of the O-H stretch and O-H wag bands are coupled, and that a lowering of the O-H stretch frequency results in an increase of the O-H wag frequency. By relating the low and high frequency parts of the corresponding O-H stretch band, we find that the sum of the O-H stretch and O-H wag frequencies falls into the range $4100\text{--}4300\text{ cm}^{-1}$. This sum corresponds well to the high frequency band centered at 4250 cm^{-1} in the IR spectra and supports previous suggestions that this band is a combination of an O-H wag and an O-H stretch mode.^{13,28}

Based on first-principles calculations we have previously suggested that the broadening of the O-H stretch band toward lower frequencies upon increasing In concentration results from a larger fraction of protons in the vicinity of dopant atoms and/or oxygen vacancies.¹³ In these nonsymmetrical configurations of the protons, e.g., Zr-OH-In and Zr-OH-In-vacancy, the In atom and the oxygen vacancy act as charged defects that tilt the proton toward a neighboring oxygen. This results in an increased tendency for strong hydrogen bond formation between the proton and the neighboring oxygen (O-H \cdots O), which lowers the O-H stretch frequency.¹³ Thus, since we now know that a lowering of the O-H stretch frequency is accompanied by a simultaneous increase of the corresponding O-H wag mode, we can relate the increased weight of the high frequency part of the O-H wag band in the INS spectra in Fig. 1 to an increased fraction of protons in strongly hydrogen bonding configurations. Importantly, the number of Zr-OH-In configurations will always be largest for $x=0.50$, while the number of configurations of protons close to oxygen vacancies, i.e., (Zr/In)-OH-(In/Zr)-vacancy, increases linearly with increasing In concentration since the degree of hydration is the same for all compositions. Thus, the fact that the relative intensities of the two high frequency Gaussians at ~ 1070 and $\sim 1250\text{ cm}^{-1}$, related to strongly hydrogen bound protons, increase steadily with increasing In concentration suggests that these bands are, at least for high dopant concentrations, related to protons in sites close to oxygen vacancies. Furthermore, apart from an electrostatic effect on the proton, the doping leads to local distortions, such as tilting of the oxygen octahedra.²⁵ It is hence reasonable to assume that in such sites the proton is additionally tilted toward a neighboring oxygen and hence experiences even stronger hydrogen bonding. The fact that the threshold for strong local structural distortions introduced by the dopant atoms may lie between $x=0.10$ and $x=0.25$ (Ref. 25) suggests that the third component at high frequency, $\sim 1250\text{ cm}^{-1}$, needed for the peak fit of the O-H wag band for $x=0.50$ and $x=0.75$ is related to such configurations of the proton.

Regarding the temperature dependence of the O-H wag band, the main effect is evidently a slight broadening with increasing temperature from 30 to 200 K, above which the broadening becomes more pronounced, as seen in Fig. 4. According to the properties of the INS band intensity [see Eq. (1)], this implies that there is only a small change of the Debye-Waller factor as the temperature is raised from 30 to 200 K, while at 300 K it is somewhat larger. This in turn

suggests that the total root mean square displacement U_T increases only slightly within the temperature 30–200 K, and then increases somewhat more strongly. The weak temperature dependence of U_T between 30 and 200 K, in particular, suggests that there is largely no difference between the proton dynamics at 30 and 200 K in this material. Since it is at 30 K unlikely that the protons are diffusing over several unit cells, this result suggests that this is also the case at 200 K. Even though U_T is larger at 300 K, it is still likely that this temperature is too low for the protons to undergo long-range diffusion. This is in agreement with a recent quasielastic neutron scattering study²⁹ of $\text{BaZr}_{0.90}\text{A}_{0.10}\text{O}_{2.95}$ ($A=Y$ and Sc), and with the very low proton conductivity as reported for the $x=0.25$ and $x=0.75$ materials^{17,18} and for proton conducting perovskites, in general, at these temperatures.³

Our findings may be compared to the INS spectra of $\text{SrCe}_{0.95}\text{M}_{0.05}\text{O}_{3-x/2}$ ($M=\text{Sc}, \text{Ho}$), for which two well separated O-H wag bands, at ~ 600 and $\sim 900\text{ cm}^{-1}$, are found even though the dopant concentration is low.¹⁴ The structures of these materials are, however, orthorhombic and not cubic, wherefore the presence of two well separated O-H wag bands most likely results from the presence of two non-equivalent oxygens as sites for the proton. It is reasonable to assume that the frequency of the O-H wag mode depends on which of the oxygens the proton is bound to. The INS spectrum of $\text{SrCe}_{0.95}\text{Sc}_{0.05}\text{O}_{3-x/2}$ is also different from the INS spectrum of $\text{BaIn}_x\text{Zr}_{1-x}\text{O}_{3-x/2}$ ($x=0.20$) in the sense that a clearly stronger effect of temperature is observed.¹⁴ Here, the 900 cm^{-1} band, which was associated with protons close to dopant atoms, decreased gradually in intensity with increasing temperature and finally disappeared into the background at 200–300 K.¹⁴ The fact that the 600 cm^{-1} band does not simultaneously increase in intensity as the 900 cm^{-1} band decreases in intensity shows that there is no redistribution of protons between the two sites. Instead, this result indicates that the protons associated to the 900 cm^{-1} band start to diffuse on increasing temperature, in contrast to our results of $\text{BaIn}_x\text{Zr}_{1-x}\text{O}_{3-x/2}$ ($x=0.20$).

The insight into the O-H wag band can be related to the actual proton conductivity of $\text{BaIn}_x\text{Zr}_{1-x}\text{O}_{3-x/2}$. From the linear fit of the total intensity of the O-H wag band in Fig. 3(c) we determine that the concentration of protons increases by a factor of 3 between $x=0.25$ and $x=0.75$. This can be compared to the corresponding increase in bulk proton conductivity by a factor of ~ 3.4 for the same materials.^{17,18} Evidently, the bulk proton conductivity scales well with the total concentration of protons in the material. This suggests that the average mobility of protons in the perovskite structure is largely the same independent of the dopant level. In this context, we relate the proton conductivity to protons experiencing different degrees of hydrogen bonding. Considering Fig. 3 we note that the absolute intensity of the 800 cm^{-1} band, related to weakly or intermediately hydrogen bound protons, increases by a factor of ~ 2.3 while each of the 1070 and 1250 cm^{-1} bands, related to strongly hydrogen bound protons, increases roughly by a factor of 10 between $x=0.20$ and $x=0.75$. The fact that the 800 cm^{-1} band scales much better to the reported proton conductivities than the 1070 and 1250 cm^{-1} bands may indicate that it is actually

those protons that are experiencing weak or intermediate hydrogen bonding that are predominantly contributing to the proton conductivity in hydrated perovskites.

VI. CONCLUSIONS

In a systematic study we have investigated the O-H wag vibrations in hydrated $\text{BaIn}_x\text{Zr}_{1-x}\text{O}_{3-x/2}$ ($x=0.20-0.75$), using inelastic neutron scattering. Our results show that the O-H wag vibrations are manifested as a strong and broad band between 600 and 1300 cm^{-1} . On increasing the In concentration the total intensity of the O-H wag band increases as a result of the increasing proton concentration. Simultaneously, the high frequency part becomes successively more and more pronounced as a consequence of an increased fraction of protons in strongly hydrogen bonding configurations,

such as close to oxygen vacancies, which act as charged defects, and by structural distortions introduced by the dopant atoms. Furthermore, we find that the mean square displacement of the protons increases only slightly as the temperature is raised from 30 to 300 K, and that the proton conductivity of hydrated $\text{BaIn}_x\text{Zr}_{1-x}\text{O}_{3-x/2}$ ($x=0.20-0.75$) scales well with total concentration of protons in the structure, suggesting that the average mobility of the protons is independent on the dopant level.

ACKNOWLEDGMENTS

This work was supported by the Swedish Research Council and National Graduate School in Material Science. Allocated beam time at the inelastic neutron spectrometer TOSCA at the ISIS Facility at the Rutherford Appleton Laboratory, UK, is gratefully acknowledged.

*maths@fy.chalmers.se

¹T. Takahashi and H. Iwahara, *Rev. Chim. Miner.* **17**, 243 (1980).

²H. Iwahara, T. Esaka, H. Uchida, and N. Maeda, *Solid State Ionics* **3-4**, 359 (1981).

³K. D. Kreuer, *Annu. Rev. Mater. Res.* **33**, 333 (2003).

⁴R. Hempelmann, C. Karmonik, T. Matzke, M. Cappadonia, U. Stimming, T. Springer, and M. A. Adams, *Solid State Ionics* **77**, 152 (1995).

⁵T. Matzke, U. Stimming, C. Karmonik, M. Soetramo, R. Hempelmann, and F. Güthoff, *Solid State Ionics* **86-88**, 621 (1996).

⁶M. Pionke, T. Mono, W. Schweika, T. Springer, and H. Schober, *Solid State Ionics* **97**, 497 (1997).

⁷W. Münch, G. Seifert, K. D. Kreuer, and J. Maier, *Solid State Ionics* **97**, 39 (1997).

⁸K. D. Kreuer, W. Munch, U. Traub, and J. Maier, *Ber. Bunsenges. Phys. Chem.* **102**, 552 (1998).

⁹W. Münch, G. Seifert, K. D. Kreuer, and J. Maier, *Solid State Ionics* **86-88**, 647 (1996).

¹⁰F. Shimojo, K. Hoshino, and H. Okazaki, *J. Phys. Soc. Jpn.* **66**, 8 (1997).

¹¹M. E. Björketun, P. G. Sundell, G. Wahnström, and D. Engberg, *Solid State Ionics* **176**, 3035 (2005).

¹²K. D. Kreuer, *Solid State Ionics* **125**, 285 (1999).

¹³M. Karlsson, M. E. Björketun, P. G. Sundell, A. Matic, G. Wahnström, D. Engberg, L. Börjesson, I. Ahmed, S. G. Eriksson, and P. Berastegui, *Phys. Rev. B* **72**, 094303 (2005).

¹⁴C. Karmonik, T. J. Udovic, R. L. Paul, J. J. Rush, K. Lind, and R. Hempelmann, *Solid State Ionics* **109**, 207 (1998).

¹⁵P. Berastegui, S. Hull, F. J. García-García, and S. G. Eriksson, *J. Solid State Chem.* **164**, 119 (2002).

¹⁶A. Manthiram, J. F. Kuo, and J. B. Goodenough, *Solid State Ionics* **62**, 225 (1993).

¹⁷I. Ahmed, S. G. Eriksson, E. Ahlberg, C. S. Knee, P. Berastegui, L. G. Johansson, H. Rundlöf, M. Karlsson, A. Matic, L. Börjesson, and Dennis Engberg, *Solid State Ionics* **177**, 1395 (2006).

¹⁸I. Ahmed, S. G. Eriksson, E. Ahlberg, C. S. Knee, M. Karlsson, A. Matic, D. Engberg, and L. Börjesson, *Solid State Ionics* **177**, 2357 (2006).

¹⁹J. B. Goodenough, J. E. Ruiz-Diaz, and Y. S. Zhen, *Solid State Ionics* **44**, 21 (1990).

²⁰S. F. Parker, J. Tomkinson, A. J. Ramirez-Cuesta, and D. Colognesi, *The TOSCA User-Guide* (ISIS Facility, Rutherford Appleton Laboratory, 2006).

²¹NIST Center for Neutron Research, 2007, www.ncnr.nist.gov.

²²B. Schrader, *Infrared and Raman Spectroscopy* (VCH Verlagsgesellschaft, Weinheim, 1995).

²³D. Colognesi, M. Celli, F. Cilloco, R. J. Newport, S. F. Parker, V. Rossi-Albertini, F. Sacchetti, J. Tomkinson, and M. Zoppi, [Suppl.] **74**, S64 (2002).

²⁴P. C. H. Mitchell, S. F. Parker, A. J. Ramirez-Cuesta, and J. Tomkinson, *Vibrational Spectroscopy with Neutrons—With Applications in Chemistry, Biology, Materials Science and Catalysis* (World Scientific Publishing, Singapore, 2005).

²⁵M. Karlsson, A. Matic, C. S. Knee, I. Ahmed, S. G. Eriksson, and L. Börjesson, arXiv:0802.0790 (unpublished).

²⁶J.-C. Li, C. Burnham, A. I. Kolesnikov, and R. S. Eccleston, *Phys. Rev. B* **59**, 9088 (1999).

²⁷K. D. Kreuer, S. Adams, W. Münch, A. Fuchs, U. Klock, and J. Maier, *Solid State Ionics* **145**, 295 (2001).

²⁸M. Glerup, F. W. Poulsen, and R. W. Berg, *Solid State Ionics* **148**, 83 (2002).

²⁹M. Karlsson, A. Matic, D. Engberg, M. E. Björketun, M. M. Koza, I. Ahmed, G. Wahnström, P. Berastegui, L. Börjesson, and S. G. Eriksson, arXiv:0802.0924 (unpublished).